Damascus University Journal for the Basic Sciences
Vol 41 No.2 (2025): 171 -159

مجلة جامعة دمشق للعلوم الأساسية
مجلد 41-عدد 2 (2025): 159- 171

Numerical study on deuteron beams properties generated from dense plasma focus devices in terms of D_2 gas pressure using Lee model code

Abdaljalil Muheialdeen Altarabulsi [1,*] Yousef Mahmood Abou-Ali [2], Sami Mustafa Alsheikh Salo Alsheikh Salo[3]

[1]Master student, Damascus University, Physics, abdaljalil.altarabulsi94@damascusuniversity.edu.sy

[2]Associate Professor, Damascus University, Experimental Plasma Physics (X-ray Laser), y.abouali@damascusuniversity.edu.sy

[3]Main Researcher, Atomic Energy Commission (AEC), Plasma Modeling, sami.salo@damascusuniversity.edu.sy

Abstract

Using Lee model code (RADPFV5.16FIB), numerical experiments on deuteron beams properties emitted from five Dense Plasma Focus (DPF) devices (PF1000, TAMU, UNU-ICTP, NX2T, PF400) were performed and compared with each other at low- and high-pressures in a range (1-15 Torr). Full details of the fitting process of the measured and computed currents and deuterons properties as function of pressure for UNU-ICTP DPF device were presented. Comparisons of I_{pinch} and *flux* in terms of pressure among the deuterons emitted from the five devices were computed and investigated to understand the behavior of the ion beam properties when the pressure varies from low to high values. For each device, the properties of the emitted deuterons such as flux, fluence, flux energy, fluence energy, ion beam current density, ion beam current, damage factor, and the energy of deuterons at fitted pressure values were presented and compared to each other. The results of this work are very significant as benchmark references in many industrial applications related to materials processing using plasma focus.

Received :2023/03/07
Accepted:2023/05/30

Keywords: Lee Model Code, Deuteron beams, Dense plasma focus devices.

ISSN (online): 2789-6366
http://journal.damascusuniversity.edu.sy/index.php/index/index

دراسة عددية لخصائص حزم الديوترونات الصادرة من أجهزة البلازما المحرقية الكثيفة بدلالة ضغط غاز D_2 باستخدام كود نموذج لي

عبد الجليل محي الدين الطرابلسي*[1]، يوسف محمود أبو علي[2]، سامي مصطفى الشيخ سلو[3]

[1] طالب ماجستير، جامعة دمشق، فيزياء، جامعة دمشق،
abdaljalil.altarabulsi94@damascusuniversity.edu.sy

[2] أستاذ مساعد دكتور، جامعة دمشق، فيزياء البلازما التجريبية (ليزر الأشعة السينية)،
y.abouali@damascusuniversity.edu.sy

[3] باحث رئيسي، هيئة الطاقة الذرية، نمذجة بلازما، sami.salo@damascusuniversity.edu.sy

الملخص

باستخدام كود نموذج لي (RADPFV5.16FIB)، أُجريَت تجارب عددية لخصائص حزم الديوترونات الصادرة من خمسة أجهزة بلازما محرقية كثيفة (PF1000, TAMU, UNU–ICTP, NX2T, PF400) وقورنت مع بعضها البعض عند ضغوط منخفضة ومرتفعة ضمن مجال (1–15 Torr). عُرضت تفاصيل كاملة لكل من عملية الموائمة للتيارين المقاس والمحسوب وخصائص الديوترونات كتوابع للضغط من أجل جهاز البلازما المحرقية الكثيفة UNU–ICTP. كذلك أُجريَت مقارنة بين التيار I_{pinch} والتدفق بدلالة الضغط للديوترونات الصادرة من الأجهزة الخمسة لفهم سلوك خصائص الحزمة الأيونية عندما يتغير الضغط من قيم منخفضة إلى قيم مرتفعة. من أجل كل جهاز، تم عرض خصائص الديوترونات الصادرة مثل التدفق والتدفق السطحي وطاقة التدفق وطاقة التدفق السطحي وكثافة تيار الحزمة الأيونية وتيار الحزمة الأيونية ومعامل الضرر وطاقة الديوترونات عند قيم الضغط المستخدمة في الموائمة بين التيارين المقاس والمحسوب وقُورنت مع بعضها البعض. تعتبر نتائج هذاالعمل مهمة جدًا كنتائج معيارية في العديد من التطبيقات الصناعية المتعلقة بمعالجة المواد باستخدام البلازما المحرقية.

الكلمات المفتاحية: كود نموذج لي، حزم ديوترونات، أجهزة بلازما محرقية كثيفة، الحزمة الأيونية.

تاريخ الإيداع: 2023/03/07
تاريخ الموافقة: 2023/05/30

1. Introduction

Dense plasma focus devices are tools used to study high-density plasmas. They confine plasma in a cylindrical chamber using high voltage electrical discharges between electrodes. This creates a fast compression of the plasma, reaching high densities and temperatures of several million Kelvin, but only for nanosecond durations. The high densities, temperatures and energy achieved make dense plasma focus devices useful for studying phenomena like dense plasma physics, fusion and generation of intense particle beams, where many researchers try to optimize the design and operating parameters to improve the performance of these devices.
The Lee model code was developed by Prof. Sing Lee as a simple computational model to describe the plasma dynamics in dense plasma focus devices. The model makes approximations like axial symmetry, one-dimensional geometry. Despite the simplifications, the Lee model code is found to reasonably predict important global parameters of the discharge like the focus point, pinch current, neutron yield and energetic particles. It thus provides a useful tool to understand plasma formation and compression in dense plasma focus devices in a conceptual way, and to optimize the device design and operating conditions for better performance, additionally to study the radiations that emit from the plasma focus. That gives a broad overview of the main concepts regarding dense plasma focus devices, what they are used for, and how the Lee model code provides a simplified computational tool to describe their plasma dynamics. In this work, an investigation and simulation were examined to study the ion beams emitted from five dense plasma focus devices, to provide the experts benchmarks references in order to help them with the experimental procedures required for the plasma applications in the field of material science and its applications.

2. Literature Review

Dense Plasma Focus (DPF) devices are pulsed sources of neutrons (Ł. Marciniak *et al*, 2018) (M. Akel et al, 2019), electron beams (P. Kubes *et al*, 2019) (P. Kubes *et al*, 2021b), soft X-ray radiation (M. A. Malek *et al*, 2019) (M. A. Mohammadi *et al*, 2020) and ion beams (S. Lee *et al*, 2012b) (S. Lee *et al*, 2013). The column plasma pinch in a DPF device typically produces pulsed ions from several of 100 keV to several of MeV (L. Bertalot *et al*, 1980) (A. Mozer *et al*, 1982) (M. Sadowski *et al*, 1988). Ion energies in DPF devices depend on capacitor bank energy, voltage, pinch current, gases, gas pressure, materials, and geometry of devices. Numerous researches have investigated the properties of ion beams experimentally (M. Etminan *et al*, 2021) (L. Bertalot *et al*, 1980) (A. Mozer *et al*, 1982) and numerically (S. Lee *et al*, 2012b) (V. A. Gribkov *et al*, 2007) using Lee model code as a virtual machine to compute the properties of ion beams such as energy, density, flux, fluence, and plasma stream specifications (S. Lee *et al*, 2012b) (S. Lee *et al*, 2013) due to its importance in several applications.
Space- and time-resolved of high energy deuterons generated from three DPF devices were studied (M. Sadowski *et al*, 1985). Ion beam has been monitored by using Faraday Cup (FC) as a detector for charged particles alongside ion Time of Flight (ToF) measurements (H. Kelly *et al*, 1998) (H. Ito *et al*, 2011) (S. J. Pestehe *et al*, 2014). The ion energies are largely in tens to hundreds of keV range, the pulse durations are tens of ns, and the currents are typically tens of kA (V. A. Gribkov *et al*, 2007). Fast deuterons of energies about 100 keV (P. Kubes *et al*, 2021a) and protons with energies about 3 MeV (A. Malinowska *et al*, 2008) both were studied using diagnostic tools which are pinhole cameras equipped with solid-state nuclear track detectors (SSNTD). Furthermore, fast ions were studied using Lee model code, with an agreement between the computed beam ion numbers and energy for numerous machines such as PF2 (S. Lee *et al*, 2012b) (S. Lee, 2014) and PF1000 (V. A. Gribkov *et al*, 2007). The measured ion current density, ion number density, ion energy and energy of flux are measured to compare reasonably well with the calculated values using Lee model code (M. Akel *et al*, 2017) (S. R. Mohanty *et al*, 2007) (M. Hassan *et al*, 2007). Published data using time resolved Schlieren imaging in the PF-400J (L. Soto *et al*, 2014) were compared with the computed results of the Lee model code for post-focus pinch fast plasma stream (FPS) speeds and stream energy, power flow density, and damage factor are agreed reasonably with all the measured quantities (M. Akel *et al*, 2016). The Lee model code is used for the comparison between the computed and monitored properties for ion beams emitted from DPF devices using various gases (V. Damideh *et al*, 2019) (V. Damideh *et al*, 2017) (M. Akel *et al*, 2022). Extensive and systematic measurements were measured using FC, PIN diode detectors, and photomultiplier-scintillator measurements to study ion beams emitted from PF machines operated with deuterium, neon, and argon gases (V. Damideh *et al*, 2019) (V. Damideh *et al*, 2017). In addition, the effect of the atomic number on the properties of the ion beams with three different gases (He, N2, Ar) was studied and compared to the calculations using Lee model code (M. Akel *et al*, 2022).

Lee code (S. Lee, 2013c) couples the electric circuit parameters with the thermodynamic, dynamic, and radiation emitted form pinch column of plasma focus. This code has been configured in 1983 (S. Lee, 1983) and used to design Mather-Type PF devices (S. Lee *et al*, 1988) (S. P. Moo *et al*, 1991). And then improved to five-phase code by adding a small finite disturbance speed (S. Lee, 2013c) (D. E. Potter, 1971). The radiation and radiation-coupled dynamics was used (A. Serban *et al*, 1997) (M. Liu *et al*, 1998) (S. Lee *et al*, 1998), then the model was published in 2000 (S. Lee, 2013b). Later, in 2007, the plasma self-absorption was included (S. Lee, 2013b) (S. Lee, 2013a). The code is widely used as a complementary facility and a virtual device in numerous devices such as UNU-ICTP (S. Lee *et al*, 1988) (S. P. Moo *et al*, 1991), NX1 (S. Lee *et al*, 1998), NX2 (S. Lee *et al*, 1998) (D. Wong *et al*, 2007), and DENA DPF devices (V. Siahpoush *et al*, 2005), and these studies provided diagnostic reference numbers for all gases (S. Lee, 2014). The computed information includes the axial and radial dynamics of current sheath (S. Lee *et al*, 1988) (A. Serban *et al*, 1997), SXR emission and its yield (M. Liu *et al*, 1998) (S. Lee *et al*, 1998), designing of devices (S. Lee, 1983) (S. Lee *et al*, 1988), optimization of devices (S. Lee, 2013c) (S. Lee *et al*, 1988) (S. H. Saw *et al*, 2009), and developing to Filippov-type DENA (V. Siahpoush *et al*, 2005). Neutron yield calculations (S. Lee *et al*, 2008) (S. Lee, 2008), current and neutrons yield limitation (S. H. Saw *et al*, 2009) (S. Lee *et al*, 2008), neutrons saturation (S. Lee, 2009), radiative collapse in PF (S. Lee *et al*, 2012c), current step technique to enhance plasma focus (S. Lee *et al*, 2012a), and anomalous resistance data (S. Lee *et al*, 2011) (R. A. Behbahani *et al*, 2012) from current signals have been studied using Lee code. The model then has been modified and used to study ion beams emitted from DPF devices (S. Lee *et al*, 2012b) (S. Lee *et al*, 2013).

To evaluate the flux of the ion beam, S. Lee and S. H. Saw (S. Lee *et al*, 2013) have written the ion beam flux (ions per $\mathrm{m^{-2}s^{-1}}$) as follows:

$$J_b = n_b v_b \qquad (1)$$

where n_b is the number of beam ions N_b per pinch volume unit which is given by relation $V_{Pinch} = \pi r_{min}^2 z_p$ (where r_{min} is the radius of the pinch cross-section, and z_p is the effective length of column of plasma pinch); v_b is the effective speed of the beam ions.

Depending on energy conservation, S. Lee and S. H. Saw (S. Lee *et al*, 2013) derived the flux J_b from the ion Beam Kinetic Energy (BKE) and the Pinch Inductive Energy (PIE). For an ion beam has N_b ion which each ion has a mass Mm_p and effective speed v_b, then the BKE equation can be written as the follows:

$$BKE = \frac{1}{2} N_b M m_p v_b^2 \qquad (2)$$

where m_p is the proton mass, and M is the ion mass number. In fact, BKE is a partition f_e of PIE, where $BKE = f_e PIE$. The PIE can be given by the equation:

$$PIE = \frac{1}{2} L_p I_{pinch}^2 \qquad (3)$$

where L_p is the inductance of plasma pinch which is given by the relation $L_p = \frac{\mu}{2\pi} \ln\left(\frac{b}{r_{min}}\right) z_p$ and $\mu = 4\pi \times 10^{-7} Hm^{-1}$; where the radius of the cathode (the outer electrode) is (b) ; the flowed electric current through the pinch of plasma is I_{pinch} which is taken at start of pinch phase. They derived the flux J_b equation (S. Lee et al, 2013):

$$Flux\ (\mathrm{ions.m^{-2}.s^{-1}}) = J_b = 2.75 \times 10^{15} \frac{f_e}{\left(MZ_{eff}\right)^{0.5}} \frac{\ln(b/r_{min})}{r_{min}^2} \frac{I_{pinch}^2}{U^{0.5}} \qquad (4)$$

Hence, the fluence is the flux multiplied by pulse duration τ:

$$Fluence\ (\mathrm{ions.m^{-2}}) = J_b \tau \qquad (5)$$

$$Fluence\ (\mathrm{ions.m^{-2}}) = 2.75 \times 10^{15} \frac{f_e}{\left(MZ_{eff}\right)^{0.5}} \frac{\ln\left(\frac{b}{r_{min}}\right)}{r_{min}^2} \frac{I_{pinch}^2}{U^{0.5}} \tau \qquad (6)$$

The value of $f_e = 0.14$ (a partition of PIE which is converted into BKE) is equivalent to ion beam energy of $3\% - 6\%$ of the stored energy E_0 in cases when the PIE has energy $20\% - 40\%\, E_0$ as observed for low

inductance DPF devices. Since the flux as the main property is determined, the rest properties of ion beam can be computed using the following relations (S. Lee *et al*, 2013):

- **Energy of flux** ($W.m^{-2}$) is given by the relation $J_b \times eZ_{eff}U$. Where U is the plasma diode voltage equals to $3V_{max}$ (S. Lee *et al*, 2008) (S. Lee *et al*, 2008) (S. Lee, 2013), where V_{max} is the maximum induced voltage of the radially collapsing current sheath (S. Lee *et al*, 2013).
- **Power flow** (W) is given by the relation $energy\ of\ flux \times \pi r_{min}^2$, where πr_{min}^2 is the cross-section of plasma pinch.
- **Current density** ($A.m^{-2}$) is given by the equation $J_b \times eZ_{eff}$ (the ion charge).
- **Ion beam current** (A) is computed using the relation $current\ density\ \times\ cross-section\ of\ pinch.$
- **Ions number per second** ($ions.s^{-1}$) is computed using the relation $J_b \times\ cross-section\ of\ pinch.$
- **Energy fluence** ($J.m^{-2}$) is computed from $J_b \times \tau \times eZ_{eff}U$.
- **Number of ions in a beam** (ions) is computed from $fluence \times\ cross-section\ of\ pinch.$
- **Energy of beam** (J) is computed using $number\ of\ ions\ in\ beam\ \times\ cross-section\ of\ pinch.$
- **Damage factor** ($W.m^{-2}.s^{0.5}$) is computed using $J_b \times eZ_{eff}U \times \tau^{0.5}$, where the damage factor is defined as the product of power flow density with the lifetime of plasma pinch (pinch duration).

3. Numerical Experiments

The numerical experiments and the computations of the five different DPF devices (PF-1000 (V. A. Gribkov *et al*, 2007), TAMU (B. Freeman, 2007), UNU-ICTP (M. A. Malek *et al*, 2019), NX2T (M. V. Roshan *et al*, 2009), PF-400 (M. Akel *et al*, 2016)) were carried out to study the properties of deuterons as a function of pressure. The ICTP-UNU device was chosen to present the procedures of fitting process. Firstly, we configured the input file of Lee model code (RADPFV5.16FIB) using the electrical and geometric parameters shown in Table 1: where the inductance of the device is L_0; the total capacity of the capacitor bank is C_0; the reduced radius of the cathode is b; the radius of the anode is a; the effective length of the anode inside the experimental chamber is z_0; the ohmic resistance of the device is r_0; the charging voltage of the battery is V_0, the initial working gas pressure is p_0. Then we run the code to fit the computed waveform current to the measured waveform current, thus, we have obtained the Lee model parameters (f_m = 0.08, f_c = 0.7, f_{mr} = 0.45 and f_{cr} = 0.7).

Table 1: The electrical and geometric parameters of the UNU-ICTP device.

L_0 (nH)	110
C_0 (μF)	30
r_0 (mΩ)	8
p_0 (Torr)	3
b (cm)	3.2
a (cm)	0.95
z_0 (cm)	16
V_0 (kV)	13.5

The model parameters f_m and f_c are the mass and current factors of the axial phase while f_{mr} and f_{cr} are the mass and current factors of the radial phase, respectively (S. Lee, 2013a) (M. Akel *et al*, 2012). Lee model parameters consider all the physical phenomena in the plasma focus, such as the mass and current distributions, additionally to possible loses (S. Lee, 2013a). Figure 1 shows the computed and measured waveforms currents of ICTP-UNU dense plasma focus device. The computed waveform current (continuous line) is fitted well to the measured waveform current (multi spikes line) for all the important parts, and the fitting procedures were done up to the end of the radial phase (at ≈ 2 μs) and the divergence beyond this point is not important and was not considered in the model (S. Lee *et al*, 2022).

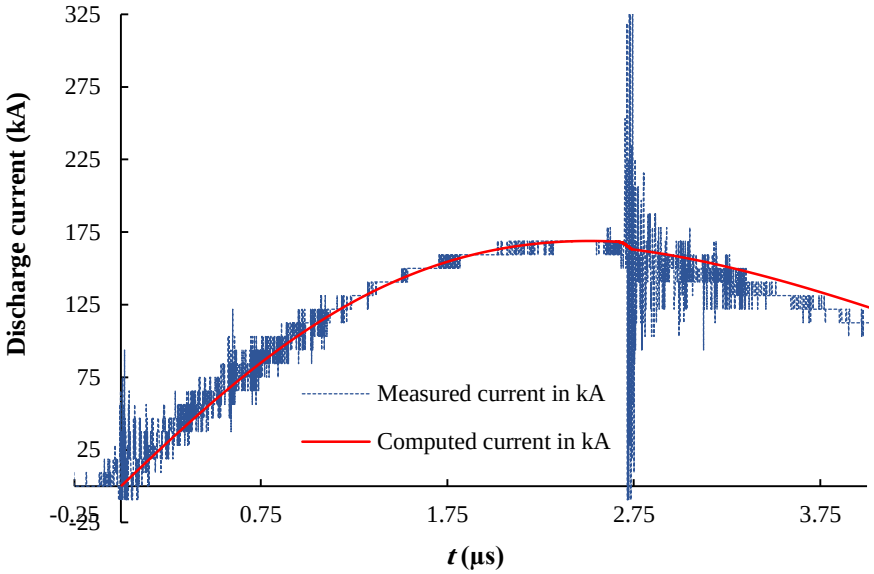

Figure 1: The measured and computed waveform currents of the 2.7-kJ UNU-ICTP device operated with 3 Torr of initial deuterium pressure.

For the rest four devices, the same computations and procedures of fitting process were repeated. Table 2 shows the electric and geometric parameters of the five PF devices, while Table 3 shows the Lee model parameters for each device.

Table 2: The electrical and geometric parameters of the five PF devices.

Device name	p_0 (Torr)	V_0 (kV)	L_0 (nH)	C_0 (μF)	r_0 (mΩ)	b (cm)	a (cm)	z_0 (cm)
PF1000-485.5 kJ	3.5	27	33.5	1332	6.3	16	11.5	60
TAMU-126 kJ	12	30	40	266.4	2.5	8.6	5.1	24
UNU-ICTP-2.7 kJ	3	13.5	110	30	8	3.2	0.95	16
NX2T-2.2 kJ	10.6	12.5	19.8	28.5	3	3.8	1.55	4
PF400-400 J	6.6	28	40	0.95	10.5	1.55	0.6	1.7

Table 3: Lee model parameters for the five PF devices.

Device name	f_m	f_c	f_{mr}	f_{cr}
PF1000-485.5 kJ	0.142	0.7	0.2	0.6
TAMU-126 kJ	0.1625	0.74	0.1944	0.6
UNU-ICTP-2.7 kJ	0.08	0.7	0.45	0.7
NX2T-2.2 kJ	0.13	0.7	0.2	0.7
PF400-400 J	0.08	0.7	0.11	0.7

4. Results and Discussion

For the UNU device, the flux and I_{pinch} were studied as function of pressure (figure 2 and 3), the flux increases with increasing of pressure until reach its peak, the peak of flux is at ($p_0 \approx 5$ Torr), then decreases with increasing of pressure because of the decrease of I_{pinch}, where the changing of flux with pressure depending on I_{pinch} strongly (see Eq.4). The relation between flux and the pressure of filled gas is attributed to the relation between gas pressure and density as well. Therefore, the gas density reduces the dynamic resistance of the current sheath, that is why I_{peak} increases when the pressure goes to high values (S. Lee *et al*, 2012c). Furthermore, the main reason of the decrease of I_{pinch} is the time matching of the focus pinch time with the current risetime of the circuit (S. Lee *et al*, 2012c). Our computations indicate that the risetime is 2.85 μs for UNU-ICTP device, therefore, after this moment, I_{pinch} starts decreasing which affects flux value at $p_0 \approx$ 5 Torr. For TAMU DPF device as a special case, it is clearly that the risetime of TAMU electrical circuit is

about 5.13 μs, therefore, we are not able to reach the maximum of I_{pinch} due to the exceeding of the experimental limits for applying very high pressures (see Figure 3).

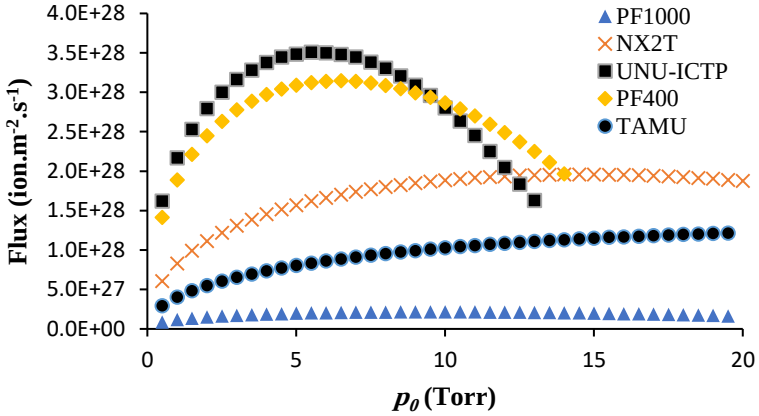

Figure 2: The flux versus pressure for the five DPF device.

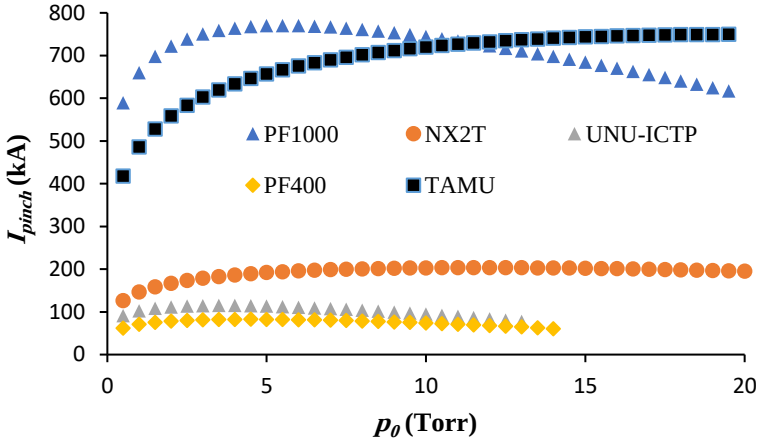

Figure 3: The I_{pinch} current versus pressure for the five DPF devices.

The simulated deuterons properties emitted from UNU-ICTP device as a function of pressure are shown in Table 4.1 and Table 4.2.

Table 4.1: Some of ion beam (deuterons) properties emitted from UNU-ICTP device versus pressure.

p_0 (Torr)	Flux (Ions.m^{-2}s^{-1}) $\times 10^{28}$	Fluence (Ions.m^{-2}) $\times 10^{20}$	En. Flux (W.m^{-2}) $\times 10^{13}$	En. Fluence (J.m^{-2}) $\times 10^{6}$	Current Density (A.m^{-2}) $\times 10^{9}$
1.00	2.2	1.8	21	1.7	3.5
2.00	2.8	2.9	23	2.4	4.5
3.00	3.2	4.0	22	2.7	5.1
4.00	3.4	4.9	20	2.9	5.4
5.00	3.5	5.7	17	2.8	5.6
6.00	3.5	6.5	15	2.7	5.6
7.00	3.4	7.1	12	2.5	5.5
8.00	3.3	7.5	9.8	2.2	5.3
9.00	3.1	7.8	7.6	1.9	4.9
10.00	2.8	7.9	5.5	1.5	4.5

Table 4.2: Some of ion beam (deuterons) properties emitted from UNU-ICTP device versus pressure.

p_0 (Torr)	Ion current (kA)	Ion Num/shot. (Ions/shot) $\times 10^{14}$	IBN (ions/s) $\times 10^{23}$	En. Beam (J)	Damage Factor ($W/m^2 s^{0.5}$) $\times 10^{10}$
1.00	18.7	9.5	1.2	9	1.9
2.00	24.4	16	1.5	13	2.3
3.00	27.9	22	1.7	15	2.4
4.00	30.3	28	1.9	16	2.4
5.00	31.9	33	2.0	16	2.2
6.00	33.0	38	2.1	16	2.0
7.00	33.6	43	2.1	15	1.8
8.00	33.9	48	2.1	14	1.5
9.00	33.9	53	2.1	13	1.2
10.00	33.6	59	2.1	12	0.92

According to the numerical experiments shown in Table 4, it is not necessary for the flux and fluence to be maximum when the I_{pinch} reaches its peak because of the effect of the pinch radius alongside pinch duration. The fluence reaches its peak at (p_0 > 10 Torr) affected by the changing of the pinch duration, pinch radius and I_{pinch}. The changing of radius pinch with pressure is attributed to radiative cooling which reduces the radius of the pinch as the pressure increases (S. Lee *et al*, 2012c). For UNU-ICTP device and for high pressures, the pinch radius will increase due to the insufficient pinch. Moreover, the increase in pressure of the filled gas reduces the speed of the current sheath through the transit from the axial to the radial phases. Therefore, the pinch duration will be longer when using high pressure due to the slowness of the current sheath movement (M. A. Malek *et al*, 2019). The energy of flux is the highest at p_0 = 2 Torr, then it decreases with higher pressure values due to the reduction of $U = 3V_{max}$ value. The energy of fluence reaches the maximum at 4 Torr, this is attributed to the relation with flux, pinch duration, and plasma diode. The ion beam current density increases with the increase of pressure until reaching 5.6×10^9 A. m^{-2} at 5.5 Torr, then reduced. Additionally, flux and ion beam current density both have the same behavior at the same value of pressure p_0 = 5.5 Torr, and that is because of the constancy of ion charge eZ_{eff} through the increase in D_2 gas pressure. The ion beam current reaches its peak at high pressure (about 8.5 Torr) and then reduces with the higher value. Moreover, the ion beam current is related to the product of the current density and pinch cross-section parameters (r_{min} and z_{max}), where z_{max} is constant approximately when pressure varies. Furthermore, we notice that the ion beam number per second and ion beam number per shot both rise to higher values with an increase of pressure till reaching the peaks at p_0 = 6 Torr and p_0 > 10 Torr, respectively. The increase of ion number per second and ion number per shot is a consequence of the rising of pinch radius r_{min}.

At 4 Torr, the energy of the ion beam has a peak with a similar behavior of ion beam number per shot. We notice that there is a difference in pressure values for the peak of the energy beam (at 4 Torr) and the peak of the ion beam number per shot (at p_0 greater than 10 Torr). The damage factor reaches its maximum at lower pressures relatively (3 Torr) and this is explained by the relation between the flux and damage factor $J_b \times eZ_{eff}U \times \tau^{0.5}$.

We have repeated all calculations for the rest four devices to demonstrate the difference in features of emitted deuterons when the pressure varies. Therefore, we summarized the flux property results in Table 5. We clearly notice that the flux has a wide range and does not depend on stored energy E_0, which means that we do not have to use high energy devices to process material since we have small devices which could emit flux with the same order or higher. Table 5 presents the flux in terms of pressure and shows that PF1000 has the lowest flux among all the other devices despite that PF1000 has the highest stored energy due to the large relative value of r_{min} shown in Table 6, while the highest flux is for PF400 DPF machine which its pinch has the smallest r_{min}. Consequently, the pinch radius is the controlling parameter despite the PF1000 device having a higher value of I_{pinch}. The divergence in flux values of devices is attributed to the divergence in r_{min}, I_{pinch}, and U values which are summarized in Table 6.

Table 5: Flux versus pressure for all devices, notice that (-) means that code stopped due to exceeding the experiment limit.

	Flux (ions.m^{-2}s^{-1}) x 10^{27}				
p_0(Torr)	PF1000	TAMU	UNU	NX2T	PF400
1.0	1.2	4	22	8.3	19
3.0	1.7	6.5	32	13	28
5.0	2.0	8.0	35	16	31
7.0	2.1	9.1	34	17	31
9.0	2.2	9.9	31	18	30
11.0	2.2	11	25	19	27
13.0	2.1	11	16	19	23
15.0	2.0	12	-	20	-

Moreover, all devices reached their peaks at a medium relatively pressures range (5-11 Torr), except TAMU and NX2T devices which reached the maximum peak at high pressure value (about 15 Torr).

Table 6: The properties of deuterons emitted from five different-energy DPF machines are sorted from the highest to the lowest stored energy. These values are computed at the fitted pressure value.

Property	PF1000 486 kJ	TAMU 126 kJ	UNU ICTP 2.7 kJ	NX2T 2.2 kJ	PF400 400 J
p_0(Torr)	3.5	12	3	10.6	6.6
I_{peak} (kA)	1840	1495	169	356	126
I_{pinch} (kA)	759	733	115	204	81
z_{max} (cm)	17.5	7.7	1.6	2.3	0.8
r_{min} (cm)	2.16	0.84	0.13	0.25	0.09
τ(ns)	216.4	78.3	12.6	24.7	5.2
V_{max} (kV)	46	65	14	21	17
Flux (ions.m^{-2}s^{-1}) $\times 10^{27}$	1.8	11	32	19	31
Fluence (ions.m^{-2}) $\times 10^{20}$	3.9	8.5	4	4.7	1.6
Ion Beam Energy (J)	12651	5923	15	94	3.1
En. Fluence (Jm^{-2}) $\times 10^{6}$	8.6	27	2.7	4.7	1.3
En. Flux (W. m^{-2}) $\times 10^{13}$	4	34	22	19	25
Power flow density (W) $\times 10^{9}$	58	76	1.2	3.8	0.59
Ion number per shot $\times 10^{14}$	5800	1900	22	95	3.8
Ion Beam Current (kA)	426.3	385.8	27.9	61.8	11.7
Current density (A.m^{-2}) $\times 10^{8}$	2.9	17	51	30	50
Dam. Fac. (W.m^{-2}s$^{0.5}$) $\times 10^{10}$	1.9	9.5	2.4	3	1.8

From Table 6 we summarized the following notes considering that each device has been operated at a fitted pressure value:

- ***Flux***: the highest is for UNU, while the lowest flux was for PF1000 device, this is attributed to the radius of pinch column r_{min} as a key parameter affected by the radiative cooling and the radiative collapse at low pressure then increases as the pressure becomes higher than a critical value (the critical value of pressure is for the smallest radius of a pinch). We should notice from Table 6 the following ratios: $\alpha = \left(\frac{I_{pinch-PF1000}}{I_{pinch-UNU}}\right)^2 = 43.56$ where $\beta = \left(\frac{r_{min-PF1000}}{r_{min-UNU}}\right)^2 = 276.07$, therefore, we can attribute the high flux of UNU-ICTP to the radius of pinch r_{min}, hence, to the radiative collapse considering the changes in the voltage of plasma diode and the radius of cathode do not play key roles due to the smallness of the ratios relatively $\gamma = \left(\frac{U_{PF1000}}{U_{UNU}}\right)^2 = 1.81$ and $\delta = \frac{\ln(b/r_{min})_{PF1000}}{\ln(b/r_{min})_{UNU}} = 0.63$.
- ***Fluence***: is related to the flux with the pinch duration, we noticed that the highest is for TAMU while the lowest is for PF400. Since most devices have the same order of flux, then, we can directly attribute the

changing of fluence to the pinch duration affected by gas pressure, which slackens the current sheath motion as its mass increases resulting in the pressure increase.

- ***Ion beam number per shot***: mainly relates to fluence and cross-section parameters which are z_p and r_{min}, the highest is for PF1000 (notice that pinch duration τ as well as the effective length of pinch z_p which have relatively large values), while the smallest is for PF400 device.
- ***Ion beam energy***: the ion beam which has a large ion number must carry high energy due to the relation of ion beam energy with the number of ions and pinch cross-section. Based on that, the highest energy is for PF1000 DPF device and the lowest is for PF400 DPF device.
- ***Energy of flux and fluence***: both relate to diode plasma voltage $U=3V_{max}$, the highest energy of flux and fluence is for TAMU while the lowest energy of fluence and flux is for PF400 and PF1000 DPF devices, respectively.
- ***Current density***: is proportional directly to J_b and Z_{eff}. Since the effective charge is constant for all devices, that means the current density increases as the flux J_b increases. The higher flux the higher current density and this leads us to UNU-ICTP device which has the highest flux, as well as PF1000 which has the smallest flux.
- ***Damage factor***: relates with U, Z_{eff}, and pinch duration τ. The highest is for TAMU device due to the large value relatively of V_{max} in addition to the small value of pinch duration. While the PF400 device has the smallest damage factor value. Since the voltage of plasma diode $U = V_{max}$ is inversely proportional with pressure while the pinch duration is directly proportional, therefore the damage factor is directly affected with pressure. However, we should mention here that all features of the ion beam are computed at the escape out moment from the plasma diode, therefore, we have to take into account the distance from the target to the plasma diode in order to calculate the effective value of the damage factor.

It is important to note that these differences in the fitted pressure values reflect the characteristics and design of each device, which can affect its performance. Such electrical parameters control the raised time of the discharge current flowing through the current sheath, while the geometric parameters control the critical quantity of gas inertia and hence controlling the travel time of the current sheath motion during the axial phase will match the raised time of the discharge current. Therefore, we would say that those differences are set as a signature for DPF device in order to make the I_{pinch} as high as possible**.**

Conclusion

For this work, we have investigated the numerical experiments on ion beam features emitted from five DPF devices using Lee model code. We have presented full details for UNU-ICTP device explaining the fitting process of the current waveforms and discussed the results of the computed properties in terms of gas pressure. The properties (*flux, fluence, energy of flux, energy of fluence, ion beam energy, power flow density, ion number per shot, ion beam current, current density, and damage factor*) as a function of initial deuterium pressure for five devices were obtained and discussed. For each device, at a constant fitted value of the gas pressure, we found that the highest flux is for UNU-ICTP device while the lowest is for PF1000 device, and we attributed these results to the relation of I_{pinch} with pressure due to the increase in the gas density alongside the pinch duration. In addition, we found that only two machines (TAMU and NX2T devices) reached their flux peaks at high pressure values (virtual values) relatively (15 Torr), while the low energy PF400 device reached its flux peak at low pressure (5 Torr), and the other peaks of the rest devices were at a range of pressure (5 – 11 Torr). We must point out of here that Lee model code has been considered as virtual DPF devices due to the agreement with the published measured ion beam features. Moreover. The Lee model code does not consider all the physics phenomena in forming plasma focus, i.e., the code does not take into account filamentation and hot-spots formation during PF discharges.

Acknowledgment

This work is financially supported by Damascus University, the Ministry of Higher Education of the Syrian Arab Republic. The authors would like to thank Director General of AECS, for encouragement and permanent support, and special thanks to Prof. Mohamad Akel (Atomic Energy Commission of Syria) for his help and many useful discussions.

References

1. Malinowska *et al*. (2008). Experimental Studies of Fast Protons Originated from Fusion Reactions in Plasma-Focus Discharges. *AIP Conference Proceedings, 993*, p. 353. doi:https://doi.org/10.1063/1.2909146
2. Mozer *et al*. (1982). Experimental studies of fast deuterons, impurity- and admixture-ions emitted from a plasma focus. *Journal of Applied Physics, 53*, 2959. doi:https://doi.org/10.1063/1.331033
3. Serban *et al*. (1997). Soft x-ray emission from a small plasma focus operated in deuterium. *Plasma Sources Science and Technology, 6*.
4. Freeman. (2007). Plasma Focus Research: Reason's for continuing efforts. In *Current trends in international fusion research - proceedings of the fourth symposium* (pp. 27-32). Canada: NRC Research. Retrieved from http:// books.google.com.my/books?isbn=0660197073
5. E. Potter. (1971). Numerical Studies of the Plasma Focus. *The Physics of Fluids, 14*, 1911. doi:https://doi.org/10.1063/1.1693700
6. Wong *et al*. (2007). An improved radiative plasma focus model calibrated for neon-filled NX2 using a tapered anode. *Plasma Sources Science and Technology, 16*.
7. H. Kelly *et al*. (1998). Analysis of the nitrogen ion beam generated in a low-energy plasma focus device by a Faraday cup operating in the secondary electron emission mode. *IEEE Transactions on Plasma Science, 26*, 113-117. doi:doi: 10.1109/27.659540
8. H. Ito *et al*. (2011). Emission characteristics of a high-energy pulsed-ion-beam produced in a dense plasma focus device. *Journal of the Korean Physical Society, 59*(61), 3674-3678.
9. L. Bertalot *et al*. (1980). Mass and energy analysis and space-resolved measurements of ions from plasma focus devices. *PHYSICS LETTERS A, 79*.
10. Ł. Marciniak *et al*. (2018). Measurements and Simulations of Neutron Emission Versus Deuterium Filling Pressure in Plasma Focus Device PF-24. *Journal of Fusion Energy, 37*, 124–129. doi:https://doi.org/10.1007/s10894-018-0157-2
11. L. Soto *et al*. (2014). Characterization of the axial plasma shock in a table top plasma focus after the pinch and its possible application to testing materials for fusion reactors. *Physics of Plasmas, 21*, 122703. doi:https://doi.org/10.1063/1.4903471
12. M. A. Malek *et al*. (2019). Optimization of neon soft X-ray yield in a low-energy dense plasma focus device. *Modern Physics Letters B, 33*, 1950077. doi:10.1142/S0217984919500775
13. M. A. Mohammadi *et al*. (2020). Experimental Study of the Effect of External Inductance on Pinch Characteristics and Neon Soft X-Ray Yield in Filippov-Type Plasma Focus Device. *Plasma Physics Reports, 46*, 696-702.
14. M. Akel, *et al*. (2019). Investigation of the Measured and Computed Neutron Yield From the PF-24 Device Operated With D2 - x%Ar Admixture. *IEEE TRANSACTIONS ON PLASMA SCIENCE, 47*.
15. M. Akel *et al*. (2016). Deuterium Plasma Focus as a Tool for Testing Materials of Plasma Facing Walls in Thermonuclear Fusion Reactors. *Journal of fusion Energy, 35*, 694–701. doi:DOI 10.1007/s10894-016-0092-z
16. M. Akel *et al*. (2017). Comparison of measured and computed beam ion current densities emitted from two 2 kJ plasma focus machines. *Vacuum, 136-c*, 163-167.
17. M. Akel *et al*. (2012). Numerical Experiments in Plasma Focus Operated in Various Gases. *IEEE Transactions on Plasma Science, 40*, 3290-3297. doi:doi: 10.1109/TPS.2012.2220863
18. M. Akel *et al*. (2022). Features of Pinch Plasma, Electron, and Ion Beams That Originated in the AECS PF-1 Plasma Focus Device. *Plasma, 5*, 184-195. doi:https://doi.org/10.3390/plasma5020014
19. M. Hassan *et al*. (2007). Nitriding of titanium by using an ion beam delivered by a plasma focus. *Journal of Physics D: Applied Physics, 40*, 769.
20. M. Sadowski *et al*. (1985). MULTI-SPIKE STRUCTURE OF ION PULSES GENERATED BY PLASMA FOCUS DISCHARGES. *Physics letters, 113 A*.
21. M. Sadowski *et al*. (1988). Ion emission from plasma-focus facilities. *Plasma Physics and Controlled Fusion, 30*, 763.
22. M. V. Roshan *et al*. (2009). Neutron and high energy deuteron anisotropy investigations in plasma focus device . *Physics of Pasmas, 16*, 053301. doi:http://dx.doi.org/10.1063/1.3133189
23. M. Liu *et al*. (1998). Soft X-ray yield measurement in a small plasma focus operated in neon. *IEEE Transactions on Plasma Science, 26*(2), 135-140. doi:10.1109/27.669614

24. M. Etminan *et al*. (2021). Angular distribution of ion beams energy and flux in a plasma focus device operated with argon gas. *Vaccum, 191*, 110352. doi:https://doi.org/10.1016/j.vacuum.2021.110352
25. P. Kubes *et al*. (2021)a. Characteristics of fast deuteron sources generated in a dense plasma focus. *The European Physical Journal Plus, 136*, 810. doi:https://doi.org/10.1140/epjp/s13360-021-01799-w
26. P. Kubes *et al*. (2021)b. Experimental Study of Fast Deuterons and Electrons in DPF Fusion Plasma. *IEEE International Conference on Plasma Science (ICOPS).* doi:doi: 10.1109/ICOPS36761.2021.9588368.
27. P. Kubes *et al*. (2019). Evolution of a Pinch Column During the Acceleration of Fast Electrons and Deuterons in a Plasma-Focus Discharge. *IEEE transactions on plasma science, 47*.
28. R. A. Behbahani *et al*. (2012). Correlation of current drop, filling gas pressure, and ion beam emission in a low energy Mather-type plasma focus device. *Journal of Applied Physics, 111*, 043304. doi:https://doi.org/10.1063/1.3686753
29. S. J. Pestehe *et al*. (2014). Dynamic Faraday cup signal analysis and the measurement of energetic ions emitted by plasma focus. *Physics of Plasmas, 21*, 033504. doi:https://doi.org/10.1063/1.4867175
30. S. Lee *et al*. (2012)a. Current-Step Technique to Enhance Plasma Focus Compression and Neutron Yield. *Journal of Fusion Energy, 31*, 603-610. doi:https://doi.org/10.1007/s10894-012-9506-8
31. S. Lee. (1983). *In Radiation in Plasmas* (Vol. 2). (B. McNamara, Ed.) Procs of Spring College in Plasma Physics (ICTP, Trieste) ISBN: 9971-966- 37-9: World Scientific, Singapore (1984).
32. S. Lee. (2008). Current and neutron scaling for megajoule plasma focus machines. *Palsma physics and controlled fusion, 50*, 14. doi:doi:10.1088/0741-3335/50/10/105005
33. S. Lee. (2009). Neutron yield saturation in plasma focus: A fundamental cause. *Applied Physics Letters, 95*, 151503. doi:https://doi.org/10.1063/1.3246159
34. S. Lee. (2013)a. *Radiative dense plasma focus computation package: RADPF*. Retrieved from http://www.plasmafocus.net; http://www.intimal.edu.my/school/fas/UFLF/ [Accessed 19 March 2023]
35. S. Lee. (2014). Plasma Focus Radiative Model: Review of the Lee Model Code. *Journal of Fusion Energy, 33*, 319-335. doi:10.1007/s10894-014-9683-8
36. S. Lee *et al*. (2012)b. Plasma focus ion beam fluence and flux—Scaling with stored energy. *Physics of Plasmas, 19*, 112703. doi:https://doi.org/10.1063/1.4766744
37. S. Lee *et al*. (2013). Plasma focus ion beam fluence and flux-For various gases. *Physics of Plasma, 20*, 062702. doi:10.1063/1.4811650
38. S. Lee *et al*. (2008). Neutron Scaling Laws from Numerical Experiments. *Journal of Fusion Energy, 27*, 292–295. doi:DOI : 10.1007/s10894-008-9132-7
39. S. Lee *et al*. (2008). Pinch current limitation effect in plasma focus. *Applied Physics Letters, 92*, 021503. doi:https://doi.org/10.1063/1.2827579
40. S. Lee *et al*. (2011). Characterizing Plasma Focus Devices—Role of the Static Inductance—Instability Phase Fitted by Anomalous Resistances. *Journal of Fusion Energy, 30*, 277–282. doi:https://doi.org/10.1007/s10894-010-9372-1
41. S. Lee *et al*. (2012)c. Numerical Experiments on Radiative Cooling and Collapse in Plasma Focus Operated in Krypton. *Journal of Fusion Energy, 32*, 42-49. doi:10.1007/s10894-012-9522-8
42. S. Lee *et al*. (1988). A simple facility for the teaching of plasma dynamics and plasma nuclear fusion. *American Journal of Physics, 56*, 62. doi:https://doi.org/10.1119/1.15433
43. S.P. Moo *et al*. (1991). An investigation of the ion beam of a plasma focus using a metal obstacle and deuterated target. *IEEE Transactions on Plasma Science, 19*(3), 515. doi:10.1109/27.87231
44. S. Lee. (2013)b. Retrieved from http://ckplee.home.nie.edu.sg/plasmaphysics/ [Accessed 25 April 2023]
45. S. Lee. (2013)c. *Institute for Plasma Focus Studies*. Retrieved from http://www.plasmafocus.net [Accessed 21 April 2023]
46. S. Lee *et al*. (1998). High rep rate high performance plasma focus as a powerful radiation source. *IEEE Transactions on Plasma Science, 26*(4), 1119 - 1126.
47. S. Lee *et al*. (2022). *Numerical Experiments Workshop on Plasma Focus (NEWPF2022)- A course on Plasma Focus Numerical Experiments.* Institute For Plasma Focus Studies (IPFS), Asian African Association for Plasma Training (AAAPT), Malaysian institute of physics, first city university college.
48. S. R. Mohanty *et al*. (2007). Effect of Anode Designs on Ion Emission Characteristics of a Plasma Focus Device. *Japanese Journal of Applied Physics, 46*, 3039.
49. S. H. Saw *et al*. (2009). Optimizing UNU/ICTP PFF Plasma Focus for Neon Soft X-ray Operation. *IEEE Transactions on Plasma Science, 37*, 1276 - 1282. doi:10.1109/TPS.2009.2022167

50. V. A. Gribkov *et al*. (2007). Plasma dynamics in the PF-1000 device under full-scale energy storage: II. Fast electron and ion characteristics versus neutron emission parameters and gun optimization perspectives. *Journal of Physics D: Applied Physics, 40*, 3592.
51. V. A. Gribkov *et al*. (2007). Plasma dynamics in PF-1000 device under full-scale energy storage: I. Pinch dynamics, shock-wave diffraction, and inertial electrode. *Journal of Physics D: Applied Physics, 40*, 1977-1989.
52. V. Siahpoush *et al*. (2005). Adaptation of Sing Lee's model to the Filippov type plasma focus geometry. *Plasma Physics and Controlled Fusion, 47*, 1065.
53. V. Damideh *et al*. (2019). Characteristics of Fast ion beam in Neon and Argon filled plasma focus correlated with Lee Model Code. *Vacuum, 169*, 108916. doi:https://doi.org/10.1016/j.vacuum.2019.108916

V. Damideh *et al*. (2017). Fast Faraday cup for fast ion beam TOF measurements in deuterium filled plasma focus device and correlation with Lee model. *Physics of Plasmas, 24*, 063302. doi:https://doi.org/10.1063/1.4985309